

# RhoA activation and actin reorganization involved in endothelial CAM-mediated endocytosis of anti-PECAM carriers: critical role for tyrosine 686 in the cytoplasmic tail of PECAM-1

Carmen Garnacho,<sup>1,2</sup> Vladimir Shuvaev,<sup>2</sup> Anu Thomas,<sup>2</sup> Lindsay McKenna,<sup>1</sup> Jing Sun,<sup>3</sup> Michael Koval,<sup>4</sup> Steven Albelda,<sup>2,3</sup> Vladimir Muzykantov,<sup>1,2,5</sup> and Silvia Muro<sup>1,2,5</sup>

<sup>1</sup>Department of Pharmacology; <sup>2</sup>Institute for Environmental Medicine; and <sup>3</sup>Pulmonary Critical Care Division of the Department of Medicine, School of Medicine, University of Pennsylvania, Philadelphia; <sup>4</sup>Division of Pulmonary, Allergy and Critical Care Medicine, Department of Medicine, Emory University School of Medicine, Atlanta, GA; and <sup>5</sup>Targeted Therapeutics Program of the Institute for Translational Medicine, School of Medicine, University of Pennsylvania, Philadelphia

**Platelet-endothelial cell adhesion molecule-1 (PECAM-1), a transmembrane glycoprotein involved in leukocyte transmigration, represents a good target for endothelial drug delivery (eg, using antibody-directed nanocarriers, anti-PECAM/NCs). Although endothelial cells do not internalize PECAM antibodies, PECAM-1 engagement by multivalent anti-PECAM conjugates and nanocarriers causes endocytosis via a nonclassic CAM-mediated pathway. We found that endothelial uptake of multivalent anti-PECAM complexes is associated with**

**PECAM-1 phosphorylation. Using model REN cells expressing a series of PECAM-1 deletion and point mutants, we found that the PECAM-1 cytoplasmic domain and, more precisely, PECAM-1 tyrosine 686, is critical in mediating RhoA activation and recruitment of EGFP-RhoA to anti-PECAM/NC binding sites at the plasmalemma, actin polymerization into phalloidin-positive stress fibers, and finally CAM endocytosis of anti-PECAM/NCs. Endothelial targeting and endocytosis of anti-PECAM/NCs were markedly efficient and did not compromise endothelial barrier function in vitro (determined by immuno-**

**staining of VE-cadherin and <sup>125</sup>I-albumin transport across endothelial monolayers) or in vivo (determined by electron microscopy imaging of pulmonary capillaries and <sup>125</sup>I-albumin transport from the blood into the lung tissue after intravenous injection of anti-PECAM/NCs in mice). These results reveal PECAM-1 signaling and interactions with the cytoskeleton, which are required for CAM-endocytosis, and may provide safe intra-endothelial drug delivery by anti-PECAM/NCs. (Blood. 2008;111:3024-3033)**

© 2008 by The American Society of Hematology

## Introduction

Endothelial cell adhesion molecules (CAMs) play an important role in blood-tissue transport, cellular recognition, signaling, and inflammation<sup>1-5</sup> and represent good candidate target determinants for drug delivery to endothelium (eg, using antibodies and antibody fragments conjugated to drugs or drug nanocarriers).<sup>6,7</sup> This is the case for platelet endothelial cell adhesion molecule-1 (PECAM-1),<sup>8</sup> a member of the immunoglobulin superfamily of transmembrane proteins, found on platelets, most leukocytes, and primarily in endothelial cells, where it concentrates at the cell-cell border.<sup>8,9</sup>

PECAM-1 consists of a 574-amino acid extracellular domain containing 6 Ig-like repeats, a short hydrophobic transmembrane domain, and a long cytoplasmic tail.<sup>10</sup> The gene for human PECAM-1, located at chromosome 17, is composed of 16 exons, with exons 3 to 8 encoding each of the 6 extracellular Ig-like domains, exon 9 encoding the transmembrane region, and 6 short exons (exons 10-16) encoding the complex cytoplasmic tail.<sup>10</sup> The extracellular region supports leukocyte anchoring and transmigration during inflammation<sup>11</sup>; hence, blocking PECAM-1 extracellular domain has anti-inflammatory effects, a secondary benefit of endothelial drug delivery strategies targeted to this molecule.<sup>6,7</sup>

Endothelial cells do not internalize anti-PECAM<sup>12</sup> or monovalent anti-PECAM scFv fusion proteins,<sup>13</sup> which thus provide drug targeting to the endothelial surface.<sup>12,13</sup> However, paradoxically, endothelial cells internalize anti-PECAM protein conjugates<sup>12</sup> and

anti-PECAM coated nanocarriers (eg, anti-PECAM/NCs) that multivalently engage the extracellular domain of PECAM-1.<sup>14,15</sup> This induces a unique vesicular transport pathway known to as CAM-mediated endocytosis,<sup>15</sup> distinct from classic mechanisms of clathrin or caveolar endocytosis, which typically operate in endothelial cells,<sup>15,16</sup> permitting intracellular drug delivery of reporter and therapeutic agents.<sup>12,14,17,18</sup>

CAM-mediated endocytosis requires signaling via the Rho-dependent kinase ROCK<sup>15,19</sup> and actin stress fiber formation,<sup>15,19</sup> suggesting signaling from PECAM-1 to the cytoskeleton after multivalent engagement of its extracellular domain. This seems somewhat similar to the central role played by Rho GTPases in the cytoskeletal changes that take place in endothelium after multivalent attachment of leukocytes to endothelial CAMs, which regulate the assembly of actin stress fibers accompanied by an increase in endothelial permeability.<sup>20</sup> However, it is unknown whether PECAM-1 engagement by leukocytes induces Rho activation.

These and some other functions of PECAM-1 are associated with rearrangements of the cellular cytoskeleton,<sup>21-27</sup> but the mechanisms that mediate these events are not well understood. It is probable that the PECAM-1 cytoplasmic domain is required to relay signals from its extracellular domain ("outside-in" signaling). For instance, reversible phosphorylation/dephosphorylation of

Submitted June 29, 2007; accepted December 18, 2007. Prepublished online as *Blood* First Edition paper, January 8, 2008; DOI 10.1182/blood-2007-06-098657.

The online version of this article contains a data supplement.

The publication costs of this article were defrayed in part by page charge payment. Therefore, and solely to indicate this fact, this article is hereby marked "advertisement" in accordance with 18 USC section 1734.

© 2008 by The American Society of Hematology

tyrosine residues 663 and 686 within an immunoreceptor tyrosine-based inhibitory motif in the PECAM-1 cytoplasmic tail has been associated to endothelial signaling, cell recognition, permeability barrier function, and flow sensing.<sup>24,25,28,29</sup> However, the role of the cytoplasmic tail in regulating PECAM-1 signaling and interactions with the endothelial cytoskeleton during CAM endocytosis, which are critical for PECAM-1-targeted drug delivery into the endothelium, remains unknown.

In this study, we explored the role of the PECAM-1 cytosolic domain in actin reorganization required for CAM-mediated endocytosis of anti-PECAM/NCs. We demonstrated that engagement of PECAM-1 by multivalent anti-PECAM complexes, but not monomolecular anti-PECAM, induced PECAM-1 tyrosine phosphorylation in endothelial cells. Using REN cells (an endothelial-like cell line derived from human mesothelioma that lacks native PECAM-1<sup>21,30</sup>) transfected with either wild-type PECAM-1 or a series of PECAM-1 cytosolic domain mutants,<sup>9,22,31-33</sup> we identified PECAM-1 cytosolic amino acid Y686 as critical for signaling leading to RhoA activation, actin stress fiber formation, and internalization of anti-PECAM/NCs. Importantly, these events leading to intracellular transport of anti-PECAM/NCs by CAM-mediated endocytosis operated in endothelial cells *in vitro* and *in vivo* without disruption of the permeability barrier, indicating the safety of this approach for endothelial drug delivery purposes.

## Methods

### Antibodies and reagents

Monoclonal antibodies to human and mouse PECAM-1 were mAb62 (a gift of Dr Nakada, Centocor, Malvern, PA) and 4G6,<sup>34</sup> and Mec13.3 (Santa Cruz Biotechnology, Santa Cruz, CA), respectively. Mouse monoclonal antiphosphotyrosine-horseradish peroxidase (HRP) (PY99) was from Santa Cruz Biotechnology. Rabbit anti-VE cadherin H72 was from Santa Cruz Biotechnology. Secondary antibodies were from Jackson ImmunoResearch (West Grove, PA). Alexa Fluor 594 phalloidin was from Invitrogen (Carlsbad, CA). Fluorescein isothiocyanate (FITC)-labeled 100-nm diameter polystyrene latex microspheres were from Polysciences (Warrington, PA). Rho activation assay kit was purchased from Upstate Biotechnology (Lake Placid, NY). All other reagents were from Sigma-Aldrich (St Louis, MO).

### Cell lines

Pooled human umbilical vein endothelial cells (HUVECs; Cambrex, East Rutherford, NJ) were maintained in culture and seeded for experiments as described.<sup>15</sup> The human mesothelioma REN cells used in this work, either those that do not express PECAM-1 or those stably transfected with human wild-type PECAM-1 (RhP) or mutant PECAM-1 isoforms, have been previously described.<sup>9,22,31-33</sup> Briefly, REN cells transfectants expressing mutant PECAM-1 were (Figure 1A):  $\Delta$ CD, lacking the entire PECAM-1 cytoplasmic domain;  $\Delta$ 11-16 and  $\Delta$ 15-16, in which these specific exons have been deleted; and Y663F or Y686F, in which tyrosine residues 663 or 686 were changed to phenylalanine.

### Preparation of multivalent anti-PECAM complexes

Multivalent anti-PECAM mAb62 conjugates (~290 nm in diameter) were prepared by crosslinking biotinylated anti-PECAM with streptavidin (90% unlabeled, 10% rhodamine labeled) as described.<sup>12,17</sup> Multivalent nanocarriers were prepared by coating anti-PECAM mAb62 on the surface of FITC-labeled 100-nm diameter polystyrene beads by surface absorption as in our prior works.<sup>14,15</sup> For *in vivo* experiments, radiolabeled anti-PECAM/NCs contained a mix of anti-PECAM Mec13.3 and <sup>125</sup>I-IgG at 95:5 molar ratio.<sup>35</sup> The effective diameter of anti-PECAM/NCs determined by dynamic

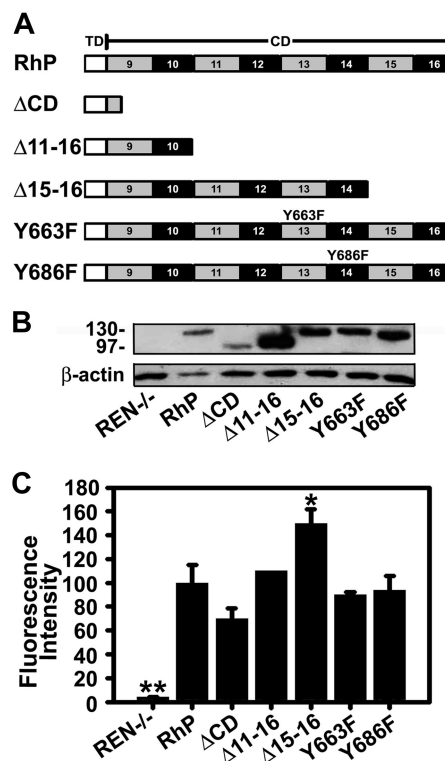


**Figure 1. Expression of human PECAM-1 isoforms by REN cells.** (A) Schematic representation of full-length PECAM-1 and different truncated and point mutant isoforms. TD indicates transmembrane domain; CD, cytoplasmic domains; RhP, full-length human PECAM-1. The 6 Ig-like extracellular domain, equal for all constructs, are not shown.  $\Delta$ CD is a construct lacking the entire PECAM-1 cytoplasmic domain.  $\Delta$ 11-16 and  $\Delta$ 15-16 are truncated constructs in which these specific exons have been deleted. Specific point mutations are shown in exons 13 and 14 for Y663F and Y686F isoforms. (B) Immunoblotting of full-length wild-type and mutant PECAM-1 isoforms expressed in REN cells. Proteins were extracted from transfected and nontransfected REN cell lysates and immunoblotted with monoclonal anti-PECAM 4G6 to human PECAM-1. Beta-actin was used as a control for protein loading. Protein molecular weight markers (in kilodaltons) are shown on the left. Nontransfected REN cells do not express PECAM-1 (REN<sup>-/-</sup>, lane 1). (C) Cell-surface expression of PECAM-1 was determined by FACS using mouse anti-human PECAM-1 monoclonal antibodies. Mean fluorescence intensity values were normalized to PECAM-1 expression level for RhP ( $n \geq 3$ ; \* $P < .01$ , \*\* $P < .001$  to RhP).

light scattering after sonication to prevent particle aggregation, was approximately 200 nm.

### PECAM-1 expression

Total PECAM-1 expression levels were determined from cell lysates of confluent REN or PECAM-1-transfected REN cells by Western blot, using 10  $\mu$ g total cell protein electrophoresed on a reducing 6% polyacrylamide gel, and then transferred to polyvinylidene difluoride membranes and blotted with mouse anti-human PECAM-1 mAb62 and HRP-conjugated goat anti-mouse antibody. PECAM-1 protein bands were quantified by densitometry using computer-assisted image analysis, and the results were corrected to  $\beta$ -actin levels, used as a loading control. Cell-surface PECAM-1 was immunostained for fluorescence microscopy and quantified by fluorescence-activated cell sorting (Flow Cytometry Facility, Wistar Institute, Philadelphia, PA) of REN or transfected REN cells, using mouse anti-human PECAM-1 mAb62 or 4G6, followed by FITC-conjugated goat anti-mouse IgG.

### PECAM-1 phosphorylation and GTPase activation

HUVECs and REN cells were incubated with control medium or medium containing monomolecular anti-PECAM antibody, or multivalent anti-PECAM/conjugates or anti-PECAM/NCs for 5 minutes, 15 minutes, or 1 hour (as indicated) at 37°C, then washed and lysed. For phosphorylation

studies, Western blot analysis was performed from total proteins separated on a 4% to 15% polyacrylamide gel, and protein bands were revealed using either HRP-mouse monoclonal antiphosphotyrosine (anti-pY) and goat polyclonal anti-PECAM followed by HRP-labeled anti-goat IgG. Activation of Rho by anti-PECAM/NCs in REN cells was assessed using a commercial pull-down kit (Rho activation assay kit, Upstate Biotechnology), which uses immunoprecipitation of activated Rho followed by Western blot analysis, according to the manufacturer's protocol. Activated Rho was normalized to total Rho in the corresponding cell lysate for each treatment.

### Endocytosis of anti-PECAM/NCs, RhoA recruitment, and cytoskeleton rearrangements

Confluent REN cells expressing wild-type PECAM-1 (RhP) or mutant PECAM-1 isoforms were incubated at 37°C for the indicated periods of time with anti-PECAM/NCs, either in control medium or medium containing 3 mM amiloride (an inhibitor of CAM-mediated endocytosis). Cells were washed, fixed in cold 2% paraformaldehyde, and stained with Texas red goat anti-mouse IgG to label noninternalized, surface located anti-PECAM/NCs. The samples were mounted on glass slides with Mowiol (EMD Chemicals, Gibbstown, NJ) and viewed with a Nikon (Melville, NY) Eclipse2000-U inverted microscope using filters optimized for FITC and Texas Red and a 40×/1.0 oil Ph3 0.17 PlanApo objective (Nikon). Images were obtained using an Orca-ICCD camera (Hamamatsu, Bridgewater, NJ), analyzed using ImagePro 3.0 software (Media Cybernetics, Silver Spring, MD), and processed with Adobe Photoshop 6.0 (Adobe Systems, San Jose, CA). With this protocol, nanocarriers bound to the cell surface are double-labeled (yellow particles) in merged fluorescence images, whereas single-labeled green particles represent internalized nanocarriers. Sonication of anti-PECAM/NCs before incubation with the cells (necessary to prevent particle aggregation, which would prevent endocytosis) renders a minor fraction of free anti-PECAM in the NC preparation, which is not endocytosed and, hence, appears as diffuse reddish staining on the cell surface. The presence of this fraction does not affect quantification of particulate anti-PECAM/NCs, which are analyzed automatically from merged images to obtain the percentage of internalized anti-PECAM/NCs with respect to the total number of particles associated to the cells.<sup>15</sup>

For assays testing RhoA recruitment to anti-PECAM/NCs binding sites in the plasmalemma, RhP or ΔCD cells were transfected using lipofectin (Invitrogen) and a vector encoding for EGFP tagged RhoA (EGFP-RhoA, a gift from Dr A. Kazi, University of Pennsylvania, Philadelphia, PA). Eight hours after transfection, the cells were incubated for 15 minutes at 37°C with nonfluorescent anti-PECAM/NCs (1 μm diameter, to enhance Rho recruitment), washed, fixed, and imaged by fluorescence microscopy.

Alternatively, to stain the actin cytoskeleton, cells were permeabilized with 0.2% Triton X-100, incubated with phalloidin conjugated to red Alexa Fluor 954, and analyzed by fluorescence microscopy to determine the increase in phalloidin-stained filamentous actin induced by anti-PECAM/NCs.

### Effects of anti-PECAM/NCs on endothelial monolayer integrity and permeability

Confluent HUVEC monolayers were incubated at 37°C with either control medium or medium containing anti-PECAM/NCs for 15 or 60 minutes, followed by fluorescent immunostaining of VE-cadherin to image effects on the endothelial cell-cell adherens junctions. Alternatively, transport of <sup>125</sup>I-labeled bovine serum albumin (BSA) across HUVEC confluent monolayers growing on 0.4-μm-pore transwell filters (from the top to the bottom chamber) was assessed in the absence or presence of either anti-PECAM/NCs or control IgG/NCs as an indication of the status of the endothelial permeability barrier. Thrombin (100 nM) served as a positive control for disruption of the monolayer integrity. Samples were mounted on glass slides with Mowiol (EMD Chemicals) and viewed with a Nikon Eclipse2000-U inverted microscope using filters optimized for FITC and Texas Red and a 40×/1.0 oil Ph3 0.17 PlanApo objective (Nikon). Images were obtained using an Orca-ICCD camera (Hamamatsu), analyzed using ImagePro 3.0 software (Media Cybernetics), and processed with Adobe Photoshop 6.0 (Adobe Systems).

### Pulmonary targeting and effects of anti-PECAM/NCs

Anesthetized C57Bl/6 male mice were injected intravenously with <sup>125</sup>I-labeled anti-PECAM or control IgG particles (~1.3 mg IgG per kg of body weight), and blood, brain, kidneys, heart, liver, lungs, and spleen were collected at death 30 minutes after injection. The radioactivity and weight of the samples were determined to estimate the accumulation of anti-PECAM/NCs versus IgG/NCs as percent of injected dose per gram of organ (% ID/g), localization ratio (LR, ID/g calculated as organ-to-blood ratio), and immunospecificity index (ISI), calculated as the LR ratio of targeted versus nontargeted NCs.

To confirm internalization of anti-PECAM/NCs by endothelial cells *in vivo*, mice injected with nonradiolabeled counterparts were perfused first with phosphate-buffered saline and then with fixative (2.5% glutaraldehyde, 4% paraformaldehyde in 0.1 M Na cacodylate buffer) through the left ventricle while maintained under ventilation, and lung samples were collected and processed for transmission electron microscopy (Biomedical Imaging Facility, University of Pennsylvania, Philadelphia, PA).

Alternatively, mice were anesthetized and injected intravenous with <sup>125</sup>I-labeled BSA in the absence or presence of either anti-PECAM/NCs or control IgG/NCs, to determine whether pulmonary accumulation of anti-PECAM/NCs causes pulmonary edema. Mice injected with tumor necrosis factorα (TNFα) (5 μg per mouse) served as a positive control for pulmonary edema. Three hours after injection, animals were killed and the radioactivity in lungs and blood isolated from the retro-orbital plexus was measured to calculate BSA lung-to-blood ratio.

All animal studies were performed in accordance with the Guide for the Care and Use of Laboratory Animals and were approved by the University of Pennsylvania IACUC committee.

### Statistics

Unless otherwise stated, the data were calculated as the mean plus or minus SD, where statistical significance was determined by Student *t* test.

## Results

### Multivalent engagement of PECAM-1 induces tyrosine phosphorylation in endothelial cells

Endothelial cells do not internalize anti-PECAM antibodies but efficiently internalize multivalent anti-PECAM complexes via CAM-mediated endocytosis,<sup>12,14,15,19</sup> a process induced by PECAM-1 cross-linking leading to actin remodeling.<sup>15,19</sup> To explore the PECAM-1 signaling mechanism associated with CAM-mediated endocytosis, we first examined phosphorylation of the PECAM-1 cytoplasmic domain in response to multivalent engagement by anti-PECAM conjugates. As shown in Figure 2, incubation of endothelial cells (HUVECs) with multivalent anti-PECAM conjugates at 37°C, but not at 4°C, caused approximately 5-fold elevation of PECAM-1 tyrosine phosphorylation, implicating tyrosine residues in PECAM-1 cytoplasmic domain in signaling for CAM-mediated endocytosis. In contrast, nonconjugated anti-PECAM antibodies, which are known not to induce endocytosis,<sup>12</sup> did not cause appreciable PECAM-1 tyrosine phosphorylation (Figure 2).

### Role of PECAM-1 cytosolic domain in endocytosis of multivalent anti-PECAM/nanocarriers

To identify motifs in the cytosolic tail of PECAM-1 that are involved in signaling during CAM-mediated endocytosis, we used multivalent anti-PECAM/NCs produced by coating anti-PECAM onto FITC polystyrene spheres. Uniform, inert, and intrinsically fluorescent multivalent anti-PECAM/NCs better serve mechanistic studies<sup>15</sup> than heterogeneous and polymorphous unlabeled anti-



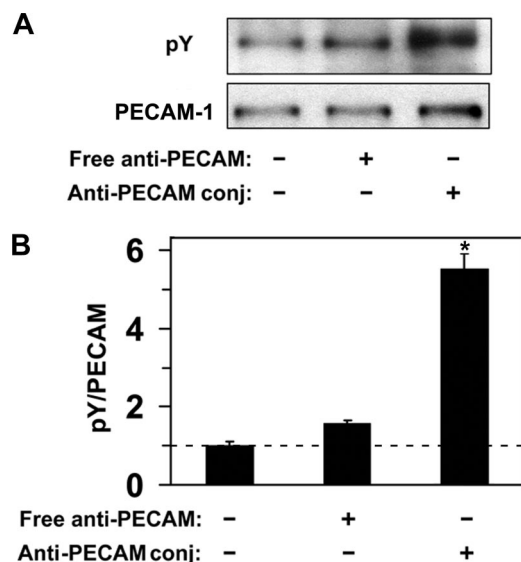


**Figure 2.** Anti-PECAM/conjugates cause PECAM-1 phosphorylation in endothelial cells. (A) HUVECs were incubated with either free anti-PECAM antibody or multivalent anti-PECAM/conjugates for 1 hour at 37°C. Cells were washed to remove nonbound conjugates, and tyrosine phosphorylation was determined from total cell lysates by Western blot using monoclonal HRP-labeled anti-pY, and goat polyclonal anti-PECAM followed by HRP-labeled anti-goat IgG. (B) Western blot densitometry. Dashed line indicates the level of PECAM-1 phosphorylation in HUVECs treated with anti-PECAM/conjugates at 4°C. Data are mean plus or minus SD ( $n = 3$ ;  $*P < .05$ ).

PECAM conjugates.<sup>14</sup> To be able to dissect PECAM-1 molecular domains responsible for signaling, we used a model consisting of human mesothelioma REN cells stably transfected to express different PECAM-1 mutants.<sup>22</sup> REN cells derived from human mesothelioma represent an appropriate model for these studies because they express some surface antigens common to endothelial cells and adopt a similar “cobblestone” morphology in culture.<sup>21,22,30</sup> Importantly, REN cells lack native PECAM-1,<sup>30</sup> which would inevitably confuse the induced responses, yet both PECAM-1 distribution (Figure S1A, available on the *Blood* website; see the Supplemental Materials link at the top of the online article) and associated signaling processes similar to endothelial cells are reconstituted after PECAM-1 expression in REN cells.<sup>32</sup>

Consistent with our previous results in endothelial cells,<sup>15</sup> anti-PECAM/NCs were rapidly internalized at 37°C by REN cells expressing full-length PECAM-1 (RhP), with half-time for maximal endocytosis less than 30 minutes (Figure 3A). Internalization was inhibited by amiloride (60.5%  $\pm$  9.2% of the control level, Figure 3B), a pharmacologic inhibitor of sodium/proton exchanger proteins (eg, NHE-1) involved in CAM-mediated endocytosis by HUVECs.<sup>15,19</sup> Hence, both endothelial and RhP cells use the same endocytic pathway for uptake of anti-PECAM/NCs, validating this cell model.

In contrast to RhP cells, anti-PECAM/NCs were not efficiently internalized by  $\Delta$ CD cells expressing a construct lacking the entire cytoplasmic domain of PECAM-1 (51.7%  $\pm$  8.8% of the control level; Figure 3A,B). Hence, the degree of inhibition of anti-PECAM/NC endocytosis in  $\Delta$ CD cells was similar to that observed in the presence of amiloride in RhP cells, directly implicating PECAM-1 cytosolic domain in CAM-mediated endocytosis.

To more precisely determine PECAM-1 cytosolic site involved in CAM-endocytosis, we used a battery of REN cells stably transfected with mutant forms of human PECAM-1 (Figure 1A), namely,  $\Delta$ 11-16 and  $\Delta$ 15-16, which represent exon deletion mutants of the cytoplasmic domain, and Y663F or Y686F point

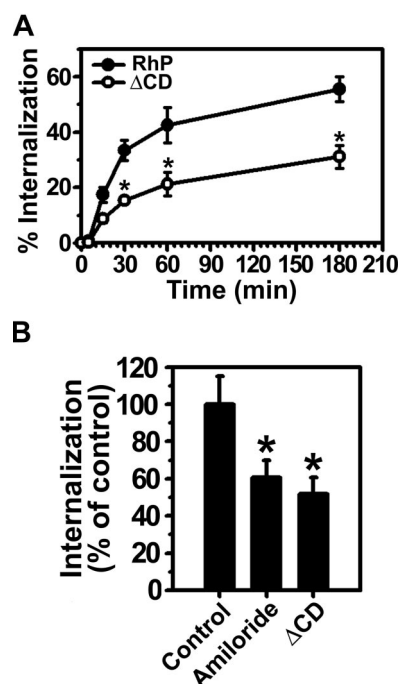


**Figure 3.** Internalization of anti-PECAM/NCs is inhibited in PECAM-1  $\Delta$ CD cells.

(A) The kinetics of internalization of FITC-labeled anti-PECAM/NCs by REN cells transfected with human wild-type PECAM-1 (RhP) (●), and PECAM-1 lacking the cytoplasmic domain ( $\Delta$ CD) (○) was determined by fluorescence microscopy after counterstaining surface nanocarriers with a Texas red secondary antibody. Internalization was quantified as the percentage of internalized anti-PECAM/NCs relative to total number of nanocarriers associated per cell. The percentage of internalized anti-PECAM/NCs was significantly lower for  $\Delta$ CD cells at each time point ( $*P < .001$ ). (B) Anti-PECAM/NC uptake was assessed in RhP and  $\Delta$ CD cells incubated with either control media or media containing amiloride, an inhibitor of CAM-mediated endocytosis. Internalization was calculated as in panel A and normalized to RhP control cells. Data are mean plus or minus SD ( $n \geq 25$  cells;  $*P < .001$ ).

mutants where tyrosine residues at the indicated amino acid positions were changed to phenylalanine. Figure 1B shows detection of PECAM-1 in cell lysates by immunoblotting. As previously reported,<sup>22,33</sup> wild-type PECAM-1 (RhP, line 2) and PECAM-1 carrying point mutations Y663F or Y686F are approximately 130 kDa. Mutant proteins missing the entire ( $\Delta$ CD) or most part PECAM-1 cytoplasmic domain ( $\Delta$ 11-16) are smaller in size (~95-100 kDa).<sup>22</sup> Untransfected REN cells represent a negative control, which does not express PECAM-1,<sup>32</sup> confirmed by negative PECAM-1 immunostaining and validating the specificity of anti-PECAM used in this study (Figure S1A).

In theory, different expression levels of PECAM-1 on the surface of transfected REN cells could lead to differences in binding anti-PECAM/NCs to cells, which could, in turn, affect endocytosis and thus confound analysis of the role of the PECAM-1 cytosolic domain in this process. To control for this, we determined cell-surface expression for each PECAM-1 mutant by FACS analysis and found that surface PECAM-1 levels for most REN-transfected cells were comparable or higher than that of REN cells expressing wild-type PECAM-1, except for  $\Delta$ CD cells, yet this difference was not statistically significant (Figure 1C). In theory, lower PECAM-1 surface expression in  $\Delta$ CD cells may have accounted for decreased endocytosis of anti-PECAM/NCs (Figure 3A). However, this scenario is unlikely because a comparable number of anti-PECAM/NCs bound per cell in  $\Delta$ CD model, compared with RhP cells (99.6%  $\pm$  8.7% of binding in RhP). Further, the significantly ( $P \leq .01$ ) higher PECAM-1 expression in  $\Delta$ 15-16 cells did not alter the level of anti-PECAM/NC binding

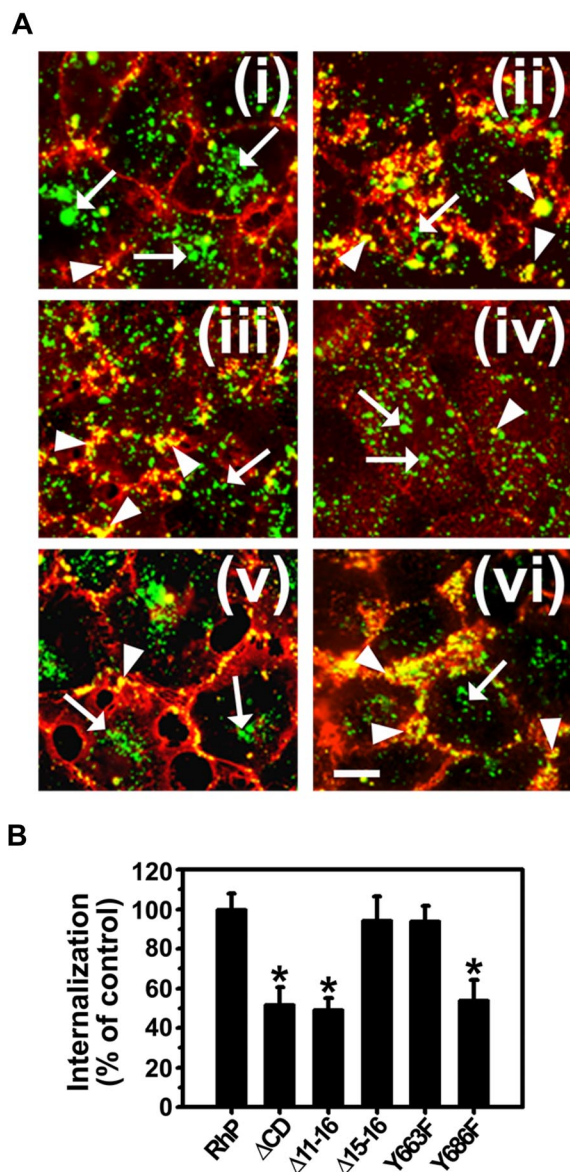


**Figure 4. Anti-PECAM/NC internalization is inhibited in REN cells expressing isoforms that lack tyrosine 686.** (A) Cells were incubated with FITC-labeled anti-PECAM/NCs at 37°C for 3 hours, washed, fixed, and counterstained with Texas red goat anti-mouse IgG to label noninternalized nanocarriers. Merged images show internalized anti-PECAM/NCs as single-labeled green particles (arrows) and surface-bound anti-PECAM/NCs as double-labeled yellow particles (arrowheads). (i) RhP. (ii) ΔCD. (iii) Δ11-16. (iv) Δ15-16. (v) Y663F. (vi) Y686F. Magnification bar represents 10 μm. (B) The percentage of internalization was calculated as mean plus or minus SD ( $n \geq 25$  cells;  $*P < .001$ ).

(100.6%  $\pm$  7.4% of binding by RhP). Notice that anti-PECAM/NCs specifically bound to PECAM-1 because they did not bind to PECAM-1-negative REN cells (0.9%  $\pm$  0.1% of binding by RhP, Figure S1B).

As shown in Figure 4, endocytosis of anti-PECAM/NCs was inhibited in Δ11-16 cells (49.4%  $\pm$  5.6% of wild-type RhP control) and Y686F cells (53.9%  $\pm$  10.4% of RhP control) at a similar level to ΔCD cells expressing PECAM-1 lacking the whole cytosolic domain (51.7%  $\pm$  8.8% of control). In contrast, for Δ15-16 and Y663F cells, endocytosis of anti-PECAM/NCs was comparable with that in RhP cells (94.3%  $\pm$  12.1% and 93.9%  $\pm$  7.9% of control, respectively). Therefore, substitution of tyrosine 686 to

phenylalanine in exon 14 was sufficient to inhibit CAM-mediated endocytosis of anti-PECAM/NCs.

#### Anti-PECAM/NCs induce Rho activation and recruitment to nanocarrier binding sites in the plasmalemma

It has been proposed that multivalent engagement of PECAM-1 can stimulate Rho-dependent kinase ROCK, an effector of the small GTPase RhoA.<sup>15</sup> To examine whether PECAM-1 engagement by anti-PECAM/NCs causes activation of RhoA, we incubated RhP and ΔCD cells with anti-PECAM/NCs at 37°C for various periods of time, and total vs activated RhoA was determined by immunoprecipitation and Western blot analysis. RhoA activity showed a 3.1-fold increase after a 15-minute incubation with anti-PECAM/NCs (Figure 5A,B). In contrast, binding of anti-PECAM/NCs to ΔCD cells had little, if any, effect on RhoA activity (Figure 5A,B). These findings suggest that signaling through PECAM-1 cytosolic domain induced by clustering PECAM-1 extracellular domain leads to RhoA activation.

Cells transfected with EGFP-RhoA were then used to determine whether RhoA is recruited to sites where PECAM-1 is engaged by anti-PECAM/NCs. Nonfluorescent, 1-μm-diameter nanocarriers were used in this experiment instead of 100-nm nanocarriers to facilitate imaging of RhoA localization to sites of carrier binding by fluorescence microscopy. Bright fluorescent rings surrounding anti-PECAM/NCs bound to the plasma membrane revealed RhoA recruitment to PECAM-1 clustering sites beneath nanocarriers in RhP cells, but not in ΔCD cells (Figure 5C vs D). Staining of filamentous actin with fluorescent phalloidin also showed colocalization of RhoA with actin stress fibers induced by anti-PECAM/NCs in RhP cells, not in ΔCD cells (Figure 5C vs D).

#### Tyrosine 686 of PECAM-1 is required for remodeling of the actin cytoskeleton induced by anti-PECAM/NCs

RhoA regulates actin cytoskeleton reorganization into stress fibers,<sup>36</sup> and filamentous actin inhibitors affect endocytosis of anti-PECAM/NCs.<sup>15</sup> To test whether PECAM-1 cytosolic domain is required for these actin rearrangements, REN cells expressing diverse PECAM-1 isoforms were incubated either in the absence or presence of anti-PECAM/NCs for 15 minutes at 37°C, followed by labeling filamentous actin with fluorescent phalloidin. Anti-PECAM/NCs did not bind to and had no effect on the actin cytoskeleton in REN cells lacking PECAM-1, where actin was predominantly organized in cortical bundles (Figure 6A top panels). Interestingly, expression of full-length PECAM-1 in REN cells (RhP cells) caused a noticeable redistribution of actin from cortical bundles into shorter cytosolic filaments. Furthermore, binding of anti-PECAM/NCs to these cells caused massive further mobilization of cortical actin into stress fibers spanning the entire cytosol (Figure 6A, RhP), enhancing phalloidin fluorescence, indicative of an increased actin polymerization into filamentous actin (Figure 6B).

REN cells transfected with PECAM mutants that showed inhibited internalization of anti-PECAM/NCs (Figure 4), namely, ΔCD, Δ11-16 and Y686F cells, showed neither actin stress fiber formation in response to anti-PECAM/NC binding (Figure 6A) nor net increased phalloidin staining (Figure 6B). In contrast, Δ15-16 and Y663F cells, which internalized anti-PECAM/NCs, also reorganized actin into stress fibers (Figure 6A) and showed enhanced phalloidin staining (Figure 6B) after incubation with anti-PECAM/NCs. Thus, Y686 in the cytosolic domain of PECAM-1 was required to stimulate actin stress fiber formation in response to anti-PECAM/NCs.



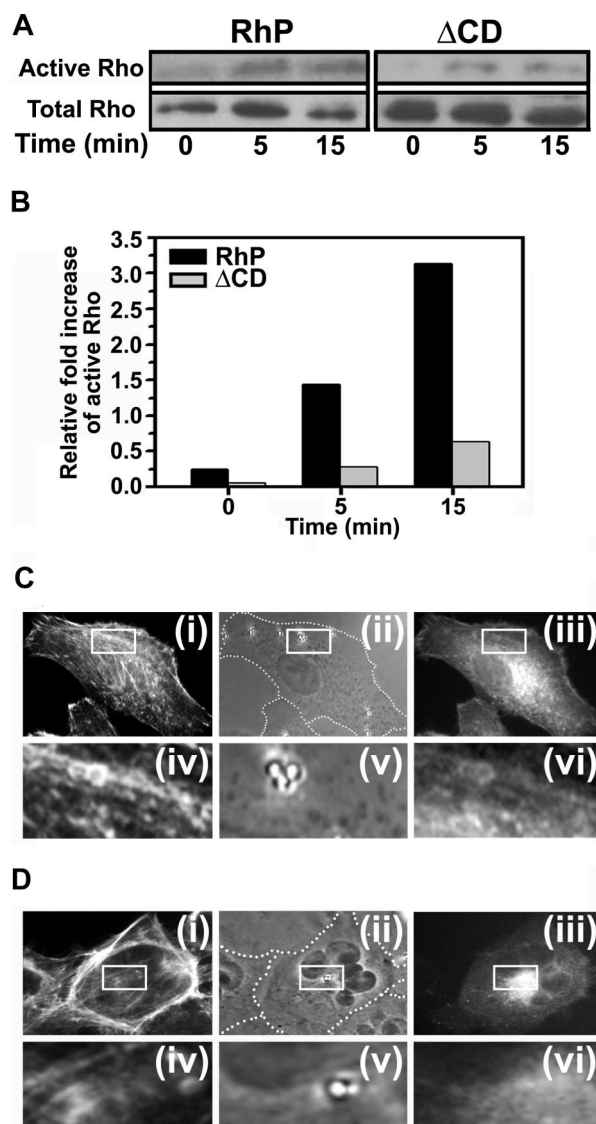


**Figure 5. PECAM-1 engagement by anti-PECAM/NCs induces RhoA activation and mobilization.** (A) RhP and ΔCD cells were incubated with anti-PECAM/NCs for 0, 5, and 15 minutes. RhoA activity was then measured using GST-RBD to pull-down active RhoA (GTP-Rho) and blotted with anti-Rho. Total Rho in cell lysates was also determined. (B) Relative RhoA activation was quantified by densitometry and indicated as fold increase of active RhoA in relation to total RhoA. RhP (C) and ΔCD (D) cells transfected to express EGFP-RhoA were incubated for 15 minutes at 37°C with 1 μm diameter, nonfluorescent anti-PECAM/NCs to visualize RhoA redistribution to nanocarrier contact-sites in RhP (Ciii) and ΔCD cells (Diii). After permeabilization, the cells were stained with red Alexa Fluor 594 phalloidin to label filamentous actin (Ci,Di). Phase contrast images (Cii for RhP and Dii for ΔCD) served to locate anti-PECAM/NCs with respect to the cell borders (marked by a dashed line). Lower panels in C and D show 4-fold magnified images of the areas outlined by the insets in RhP (Civ-Cvi) and ΔCD (Div-Dvi) cells.

#### Binding and endocytic transport of anti-PECAM/NCs do not affect integrity of endothelial monolayer in vitro and in vivo

Actin cytoskeletal reorganization and contractility mediated by Rho GTPase can potentially disrupt intercellular junctions and reduce endothelial barrier function.<sup>37</sup> In theory, actin rearrangement induced by anti-PECAM/NCs in cultured RhP cells used in this work, similar to those observed in HUVECs in our prior studies,<sup>15,19</sup> could also lead to cellular contraction and detrimental consequences on the endothelial permeability. In some pathological settings intended to be treated by drug targeting strategies, endothe-

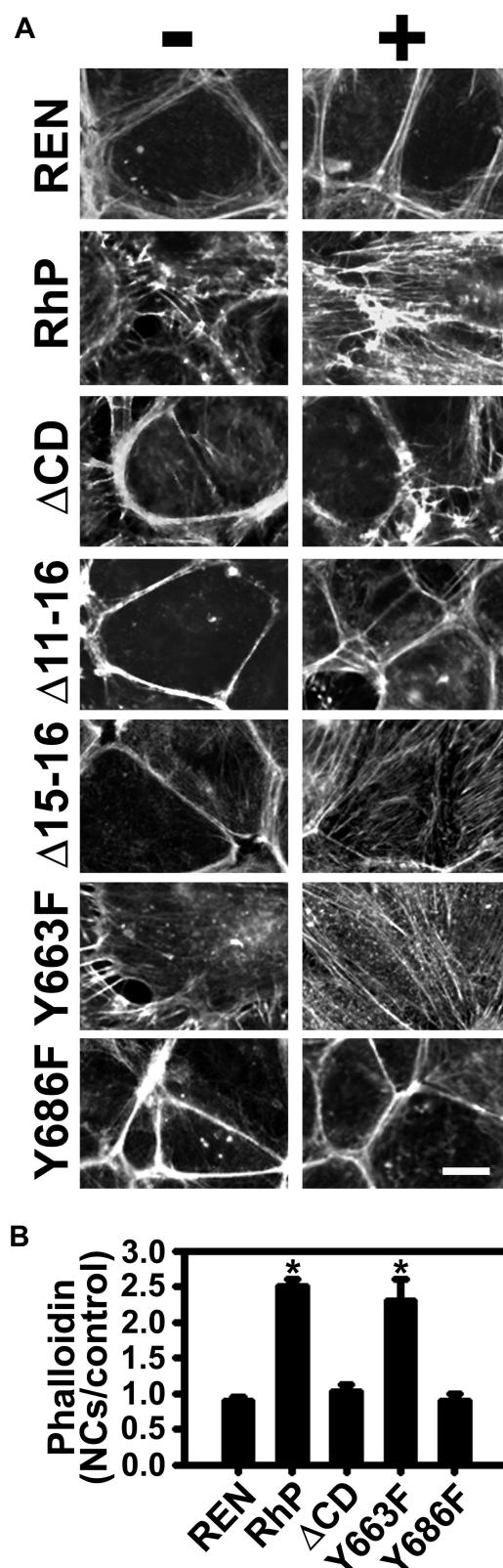


**Figure 6. Induction of actin remodeling by anti-PECAM/NCs is inhibited in REN cells expressing isoforms lacking tyrosine 686.** (A) Transfected and nontransfected REN cells were incubated either in the absence (–) or presence (+) of anti-PECAM/NCs for 15 minutes at 37°C, washed, fixed, and stained with Alexa Fluor 594 phalloidin to label filamentous actin. PECAM-1-negative REN cells were used as a control. Magnification bar represents 10 μm. (B) Quantification of fluorescent phalloidin indicative of filamentous actin, expressed as fold increase of fluorescence for each cell line after induction by anti-PECAM/NCs. Data are mean plus or minus SEM (n ≥ 10 cells; \*P < .0001).

lial permeability changes caused by anti-PECAM/NCs would represent an adverse effect.

To evaluate this key safety aspect of intra-endothelial drug delivery via PECAM-1, we first examined potential disruption of the endothelial monolayer integrity caused by anti-PECAM/NCs in cell cultures. As shown in Figure 7A, we did not detect appreciable changes in the distribution of the adherens junction marker, VE-cadherin, in HUVECs incubated with anti-PECAM/NCs. In addition, anti-PECAM/NCs (similarly to control IgG/NCs) did not increase transport of radiolabeled albumin across HUVEC monolayers grown to confluence on 0.4- $\mu$ m-pore transwell filters, whereas this was significantly enhanced by thrombin-positive control (Figure 7B), validating this method. These results indicate that the integrity of the endothelial monolayer in vitro is unaffected by anti-PECAM/NCs.

Second, we studied endothelial targeting and effects of anti-PECAM/NCs on the vascular permeability in mice. Both anti-PECAM/NCs and nontargeted control IgG/NCs were rapidly eliminated from blood ( $2.0\% \pm 0.7\%$  and  $3.6\% \pm 0.2\%$  ID/g of blood 30 minutes after injection, respectively), in part because of uptake by the reticuloendothelial system in liver and spleen (Table 1). However, anti-PECAM/NCs, but not IgG/NCs, accumulated in the lungs specifically ( $89.8\% \pm 13.8\%$  vs  $10.2\% \pm 1.1\%$  ID/g, Table 1). Indeed, lung-to-blood ratio (localization ratio, LR) of anti-PECAM/NCs versus control IgG/NCs was  $107.8 (\pm 29.7)$  versus  $2.9 (\pm 0.3)$ , Table 1).

Specific targeting of anti-PECAM/NCs versus control IgG/NCs was also detectable in the brain ( $1.0\% \pm 0.1\%$  vs  $0.4\% \pm 0.04\%$  ID/g), kidney ( $5.0\% \pm 0.3\%$  vs  $3.0\% \pm 0.3\%$  ID/g), and heart ( $5.5\% \pm 0.5\%$  vs  $2.1\% \pm 0.3\%$  ID/g, Table 1). Binding of anti-PECAM/NCs to endothelium in all of these vascular beds explains their faster blood clearance versus IgG/NCs ( $3.4\% \pm 1.7\%$  vs  $17.1\% \pm 1.4\%$  ID/g of blood 1 minute after injection), despite less profound “nonspecific” uptake in liver ( $24.7\% \pm 1.8\%$  vs  $48.9\% \pm 2.9\%$  ID/g) and spleen ( $61.7\% \pm 5.2\%$  vs  $87.9\% \pm 8.4\%$  ID/g).

In addition, transmission electron microscopy of postmortem specimens of mouse lungs collected 3 hours after injection showed that anti-PECAM/NCs were internalized in vivo by pulmonary endothelial cells ( $54.5\% \pm 12.3\%$  internalization,  $n = 15$  transmission electron microscopy micrographs), without endothelial disruption or other detectable abnormalities in the lungs (notice intact endothelial junctions in Figure 7C,CJ), despite the presence of numerous anti-PECAM/NCs accumulated.

To confirm the safety of intra-endothelial targeting of anti-PECAM/NCs and test specifically and quantitatively pulmonary vascular permeability, leakage of plasma proteins into the lung tissue was measured by injection of  $^{125}$ I-labeled albumin (Figure 7D). Injection of an inflammatory cytokine TNF- $\alpha$ , used as a positive control, caused 2-fold elevation of pulmonary uptake of  $^{125}$ I-albumin, reflecting pulmonary edema, whereas injection of anti-PECAM/NCs or control IgG/NCs caused no elevation of pulmonary vascular permeability. Thus, anti-PECAM/NCs represent a safe targeting carrier platform that may permit effective delivery of pharmacologic agents to the pulmonary vasculature.

## Discussion

PECAM-1 represents a robust target for drug delivery to either normal or pathologically altered endothelium<sup>38-40</sup> (eg, for prophylactic or therapeutic interventions).<sup>6,7,12,13,17,18,41</sup> For instance, endo-

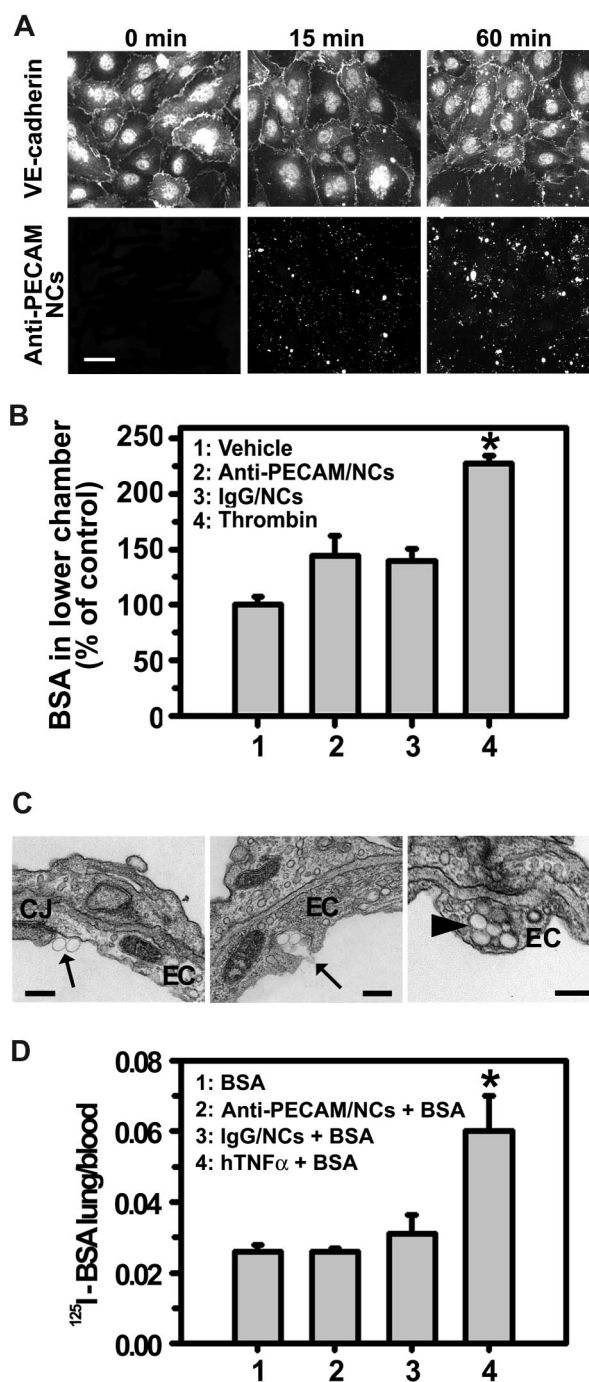


**Figure 7. Anti-PECAM/NCs targeting and effects on endothelial cells in vitro and in vivo.** (A) VE-cadherin staining in HUVECs incubated in the absence or presence of anti-PECAM/NCs at 37°C for 15 or 60 minutes. VE-cadherin (top panels) was continuously distributed around the entire periphery of control cells and cells exposed to NCs (lower panels). Magnification bar represents 20  $\mu$ m. (B) HUVECs grown on 0.4- $\mu$ m-pore transwell filters were incubated with  $^{125}$ I-labeled BSA either in the absence or presence of anti-PECAM/NCs, control IgG/NCs, or 100 nM thrombin as a positive control for barrier disruption. After incubation for 1 hour at 37°C, media in the lower chamber was collected and radioactivity measured to calculate the percentage of  $^{125}$ I-BSA transported across the endothelial monolayer with respect to total  $^{125}$ I-BSA added. Data were normalized to  $^{125}$ I-BSA transport in control cells. Data are mean plus or minus SEM ( $n = 4$  wells; \* $P < .001$ ). (C) Transmission electron microscopy of mouse lungs 3 hours after injection with anti-PECAM/NCs. Arrows indicate anti-PECAM/NCs bound to the surface of endothelial cells and being incorporated into vesicular invaginations. Arrowheads indicate anti-PECAM/NCs internalized by pulmonary endothelial cell (EC). Magnification bar represents 200 nm. (D) Lung-to-blood ratio of  $^{125}$ I-labeled BSA 3 hours after injection in mice either in the absence or presence of anti-PECAM/NCs, control IgG/NCs, or TNF $\alpha$ . Data are mean plus or minus SD ( $n \geq 4$  mice; \* $P < .05$ ).

**Table 1. Biodistribution of <sup>125</sup>I-labeled anti-PECAM/NCs versus IgG/NCs 30 minutes after intravenous injection in mice**

	Blood	Brain	Kidney	Heart	Liver	Lung	Spleen
<b>%ID/g</b>							
IgG/NCs	3.6 ± 0.2	0.4 ± 0.04	3.0 ± 0.3	2.1 ± 0.3	48.9 ± 2.9	10.2 ± 1.1	87.9 ± 8.4
Anti-PECAM/NCs	2.0 ± 0.7*	1.0 ± 0.1†	5.0 ± 0.3†	5.5 ± 0.5†	24.7 ± 1.8†	89.8 ± 13.8†	61.7 ± 5.2*
<b>LR</b>							
IgG/NCs	—	0.1 ± 0.02	0.9 ± 0.1	0.6 ± 0.1	14.3 ± 1.5	2.9 ± 0.3	25.4 ± 2.9
Anti-PECAM/NCs	—	1.2 ± 0.3*	5.5 ± 1.2†	6.1 ± 1.4†	26.4 ± 5.7	107.8 ± 29.7†	64.3 ± 13.6
ISI: Anti-PECAM: IgG	—	9.6	6.4	9.9	1.8	36.7	2.5

Data are mean SEM; n ≥ 3.

ID/g indicates percent injected dose per gram of organ; LR, localization ratio (% ID/g in an organ: % ID/g in blood); ISI, immunospecificity index (LR for anti-PECAM/NCs: LR for IgG/NCs); and —, not applicable.

\*P < .05 (Student t test).

†P < .01 (Student t test).

thelial targeting of antioxidant enzymes conjugated with anti-PECAM or anti-PECAM nanocarriers (anti-PECAM/NCs) provides therapeutic effects both in cell culture and animal models of oxidative stress.<sup>6,7,17,18</sup>

Anti-PECAM conjugates and nanocarriers are transported from the endothelial surface to intra-endothelial vesicular compartments via a nonclassic CAM-mediated endocytosis.<sup>14,15,17,42</sup> This pathway is induced by multivalent engagement of endothelial PECAM-1 and requires actin reorganization into stress fibers, which depend on the Rho effector ROCK.<sup>14,15,17,42</sup> However, the molecular regulation of these events, critically important for intracellular drug delivery, remains unknown.

In this study, we found that multivalent engagement of PECAM-1 by anti-PECAM conjugates or nanocarriers induced PECAM-1 tyrosine phosphorylation, RhoA recruitment to nanocarrier binding sites at the plasmalemma, and RhoA activation and actin polymerization into stress fibers, leading to endocytosis of anti-PECAM carriers both in cell cultures and pulmonary endothelium in vivo, without affecting the endothelial permeability barrier. Truncation of PECAM-1 cytosolic domain and point mutations of potential signaling residues located in this domain revealed a critical role for tyrosine 686 in the signaling regulating these events.

PECAM-1 tyrosine phosphorylation is involved in diverse pathways of cellular stimulation.<sup>21,27,43</sup> Endothelial PECAM-1 becomes phosphorylated in response to shear stress<sup>26,44</sup> and by exposure to hypo-osmotic or hyperosmotic media causing cell deformation.<sup>26</sup> Wound-induced cell migration also stimulates PECAM-1 tyrosine phosphorylation<sup>25</sup> in endothelial cells, and PECAM-1 crosslinking in T lymphocytes leads to tyrosine phosphorylation.<sup>45</sup>

Interestingly, the 2 immunoreceptor tyrosine-based inhibitory motifs of PECAM-1 tyrosine 663 and 686 are involved in these events.<sup>25,28,29</sup> However, only PECAM-1 tyrosine 686 has a detectable signaling function in mediating CAM endocytosis of anti-PECAM/NCs (Figures 4,6). Although the mechanisms regulating distinct signaling through PECAM-1 tyrosine residues is unknown at present, this could be explained by differential phosphorylation of tyrosine 686 versus 668, previously observed in other settings.<sup>46</sup>

Truncation of PECAM-1 cytosolic domain and, more precisely, mutation of PECAM-1 Y686 in model REN cells abrogated RhoA recruitment to anti-PECAM/NC binding sites at the plasmalemma and RhoA activation (Figure 5), actin polymerization into stress fibers (Figure 6), and nanocarrier internalization (Figures 3,4). This indicates that CAM-mediated endocytosis regulated by PECAM-1 phosphorylation requires RhoA signaling as a downstream molecu-

lar switch to turn on or off actin signal transduction. Rho proteins<sup>47</sup> have been found to regulate actin cytoskeleton, cell adhesion, endocytosis, and vesicular trafficking in endothelial cells.<sup>36</sup> Particularly, Rho activation has been associated to numerous processes involving PECAM-1, including regulation of cell-cell and cell-matrix interactions,<sup>48</sup> cytoskeletal changes induced by mechanical factors,<sup>21,26,27,49,50</sup> and leukocyte transmigration in vivo.<sup>1-5,20,51</sup>

Conceivably, PECAM-1 interaction with the cytoskeleton may regulate these endothelial functions.<sup>21-27,52,53</sup> In support of this notion, PECAM-1 associates physically and functionally with the underlying cytoskeleton: approximately 20% to 30% endothelial PECAM-1 has been found in Triton-insoluble cytoskeleton fractions,<sup>28,54</sup> which increased to approximately 65% during cell migration.<sup>28</sup> The catenins are probably candidates linking PECAM-1 and the actin cytoskeleton, yet this has not been established with certainty.<sup>27,55</sup> Perhaps PECAM-1 may also interact with the actin cytoskeleton through RhoA, as shown in Figure 5C.

Of note, we detected actin cortical bundles in PECAM-1-negative REN cells and cells that express ΔCD or Y686F PECAM-1, in contrast to wild-type or Y663F PECAM-1 associated to shorter cytosolic actin filaments (Figure 6A). ΔCD PECAM-1 does not accumulate in the cell border, it fails to engage PECAM-1 molecules in neighboring cells, and it is more abundant in the luminal surface.<sup>22,23</sup> Y686F PECAM-1 in 3T3 cells has also been associated with an altered PECAM-1 distribution during cell migration.<sup>23</sup> Perhaps the inability of ΔCD PECAM-1 to signal cytoskeleton changes may contribute to distinct trafficking and distribution of ΔCD or Y686F PECAM-1 in the plasmalemma.

Interestingly, PECAM-1 engagement by leukocytes induces recruitment of PECAM-1 molecules from plasmalemma invaginations to the endothelial cell-cell border surface.<sup>56</sup> This shallow compartment is distinct from endosomes and lysosomes, yet the mechanism by which PECAM-1 recycles between these regions is unknown. Although we observed that anti-PECAM/NCs traffic to endo-lysosomal compartments,<sup>17,42</sup> perhaps vesiculization induced by engagement of PECAM-1 with anti-PECAM/NCs is reminiscent of PECAM-1 recycling pathway.<sup>56</sup> However, in our studies in transfected REN cells and HUVECs (Figure S1), anti-PECAM and anti-PECAM/NCs locate to junctional and luminal areas on the cell surface, and we could not establish whether one of these fractions is preferentially internalized because intracellular anti-PECAM/NCs traffic to perinuclear endo-lysosomes.<sup>17,42</sup> It is plausible that PECAM-1 engagement by anti-PECAM Ab62 (known to inhibit PECAM-1 homophilic interaction<sup>5</sup>) disassembles PECAM-1 dimers at the cell-cell border causing the molecule to redistribute to the luminal surface. However, we traced anti-PECAM/NCs<sup>42</sup> (not



PECAM-1), and whether internalized PECAM-1 recycles to the plasmalemma from nascent invaginations is unknown. Interestingly, a related molecule, which also mediates CAM endocytosis after multivalent engagement by nanocarriers (ICAM-1), does not traffic with anti-ICAM/NCs to lysosomes but rather recycles to the plasmalemma after internalization.<sup>35</sup>

Anti-PECAM/NCs specifically targeted vascular endothelium in vivo (Table 1), and primarily accumulated in the pulmonary vasculature, which represents 30% of the body endothelium and receives 100% venous cardiac output.<sup>57,58</sup> The relevance of endothelial targeting by anti-PECAM/NCs for drug delivery is reflected by the fact that these particles are internalized by pulmonary endothelium in vivo (Figure 7C), without disrupting the vascular permeability (Figure 7D), similarly to cultured endothelial cells (Figure 7A,B). This is somewhat unexpected because the integrity of endothelial junctions has been shown to be compromised by vascular stress in PECAM-1-deficient mice.<sup>59-63</sup>

In addition, activation of RhoA increases actin-myosin contractility, leading to opening of intercellular junctions<sup>37</sup> and thus disruption of the endothelial barrier function. In contrast to anti-PECAM/NCs, anti-PECAM-1 F(ab')<sub>2</sub> increases transport of <sup>125</sup>I-albumin across endothelial junctions, both in cultured cell and in mice.<sup>2</sup> It is conceivable that binding of nano-scale PECAM-1 ligands permissive of CAM-mediated endocytosis favors intracellular vesicular transport, in contrast to noninternalizable anti-PECAM, its fragments, or leukocytes with diameter on the order of 10  $\mu$ m, which induce opening of intercellular junctions.

Taken together with the lack of edema and other adverse effects in numerous animal studies documenting the therapeutic effects of anti-PECAM conjugates with antioxidant drugs,<sup>17,18</sup> the present results indicate that nanocarriers directed to PECAM-1 represent an attractive platform for nondamaging intra-endothelial drug delivery. Further elucidation of the molecular mechanisms in-

volved in regulation of this process will help to better define potential utility and limits of this strategy, as well as natural role of PECAM-1 in endothelial physiology and pathology.

## Acknowledgments

The authors thank Drs Qian-Chun Yu and Neelima Shah (Biomedical Imaging Core, University of Pennsylvania, Philadelphia) for technical help with transmission electron microscopy and Dr Jeffrey Faust and Alistaire Acosta (Flow Cytometry Facility, the Wistar Institute, Philadelphia, PA) for technical help with FACS analysis.

This study was supported by American Heart Association SDG 0435181N, National Institutes of Health grants R21 HL85533, P30 DK47757-14 (S.M.), R01 HL71175, HL078785, and HL73940, and Department of Defense PR 012262 (V.M.).

## Authorship

Contribution: C.G., V.S., A.T., L.M., and J.S. performed experiments; C.G., V.M., and S.M. analyzed results; C.G. and V.S. prepared the figures; M.K., S.A., V.M., and S.M. designed the research; and C.G., M.K., S.A., V.M., and S.M. wrote the paper.

Conflict-of-interest disclosure: The authors declare no competing financial interests.

Correspondence: (re: vascular drug delivery) Vladimir Muzykantov, Institute for Environmental Medicine, 1 John Morgan Building, 3620 Hamilton Walk, Philadelphia, PA 19104-6068; e-mail: muzykant@mail.med.upenn.edu; or (re: endothelial cell adhesion molecules and endocytosis) Silvia Muro, Department of Pharmacology, John Morgan Building, 3620 Hamilton Walk, Philadelphia, PA 19104-6068; e-mail: silvia@mail.med.upenn.edu.

## References

- Muller WA, Weigl SA, Deng X, Phillips DM. PE-CAM-1 is required for transendothelial migration of leukocytes. *J Exp Med*. 1993;178:449-460.
- Ferrero E, Ferrero ME, Pardi R, Zocchi MR. The platelet endothelial cell adhesion molecule-1 (PECAM1) contributes to endothelial barrier function. *FEBS Lett*. 1995;374:323-326.
- Wakelin MW, Sanz MJ, Dewar A, et al. An anti-platelet-endothelial cell adhesion molecule-1 antibody inhibits leukocyte extravasation from mesenteric microvessels in vivo by blocking the passage through the basement membrane. *J Exp Med*. 1996;184:229-239.
- Liao F, Ali J, Greene T, Muller WA. Soluble domain 1 of platelet-endothelial cell adhesion molecule (PECAM) is sufficient to block transendothelial migration in vitro and in vivo. *J Exp Med*. 1997;185:1349-1357.
- Nakada MT, Amin K, Christofidou-Solomidou M, et al. Antibodies against the first Ig-like domain of human platelet endothelial cell adhesion molecule-1 (PECAM-1) that inhibit PECAM-1-dependent homophilic adhesion block in vivo neutrophil recruitment. *J Immunol*. 2000;164:452-462.
- Muro S, Muzykantov VR, Murciano JC. Characterization of endothelial internalization and targeting of antibody-enzyme conjugates in cell cultures and in laboratory animals. *Methods Mol Biol*. 2004;283:21-36.
- Ding BS, Dziubla T, Shuvaev VV, Muro S, Muzykantov VR. Advanced drug delivery systems that target the vascular endothelium. *Mol Interv*. 2006;6:98-112.
- Muller WA, Ratti CM, McDonnell SL, Cohn ZA. A human endothelial cell-restricted, externally disposed plasmalemmal protein enriched in intercellular junctions. *J Exp Med*. 1989;170:399-414.
- Sun J, Williams J, Yan HC, Amin KM, Albelda SM, DeLisser HM. Platelet endothelial cell adhesion molecule-1 (PECAM-1) homophilic adhesion is mediated by immunoglobulin-like domains 1 and 2 and depends on the cytoplasmic domain and the level of surface expression. *J Biol Chem*. 1996;271:18561-18570.
- Newman PJ, Berndt MC, Gorski J, et al. PE-CAM-1 (CD31) cloning and relation to adhesion molecules of the immunoglobulin gene superfamily. *Science*. 1990;247:1219-1222.
- Vaporciyan AA, DeLisser HM, Yan HC, et al. Involvement of platelet-endothelial cell adhesion molecule-1 in neutrophil recruitment in vivo. *Science*. 1993;262:1580-1582.
- Muzykantov VR, Christofidou-Solomidou M, Bal-yasnikova I, et al. Streptavidin facilitates internalization and pulmonary targeting of an anti-endothelial cell antibody (platelet-endothelial cell adhesion molecule 1): a strategy for vascular immunotargeting of drugs. *Proc Natl Acad Sci U S A*. 1999;96:2379-2384.
- Ding BS, Gottstein C, Grunow A, et al. Endothelial targeting of a recombinant construct fusing a PECAM-1 single-chain variable antibody fragment (scFv) with prourokinase facilitates prophylactic thrombolysis in the pulmonary vasculature. *Blood*. 2005;106:4191-4198.
- Wiewrodt R, Thomas AP, Cipelletti L, et al. Size-dependent intracellular immunotargeting of therapeutic cargoes into endothelial cells. *Blood*. 2002;99:912-922.
- Muro S, Wiewrodt R, Thomas A, et al. A novel endocytic pathway induced by clustering endothelial ICAM-1 or PECAM-1. *J Cell Sci*. 2003;116:1599-1609.
- Stan RV. Endocytosis pathways in endothelium: how many? *Am J Physiol Lung Cell Mol Physiol*. 2006;290:L806-L808.
- Kozower BD, Christofidou-Solomidou M, Sweitzer TD, et al. Immunotargeting of catalase to the pulmonary endothelium alleviates oxidative stress and reduces acute lung transplantation injury. *Nat Biotechnol*. 2003;21:392-398.
- Christofidou-Solomidou M, Scherpereel A, Wiewrodt R, et al. PECAM-directed delivery of catalase to endothelium protects against pulmonary vascular oxidative stress. *Am J Physiol Lung Cell Mol Physiol*. 2003;285:L283-L292.
- Muro S, Mateescu M, Gajewski C, Robinson M, Muzykantov VR, Koval M. Control of intracellular trafficking of ICAM-1-targeted nanocarriers by endothelial Na<sup>+</sup>/H<sup>+</sup> exchanger proteins. *Am J Physiol Lung Cell Mol Physiol*. 2006;290:L809-L817.
- Greenwood J, Walters CE, Pryce G, et al. Lovastatin inhibits brain endothelial cell Rho-mediated lymphocyte migration and attenuates experimental autoimmune encephalomyelitis. *FASEB J*. 2003;17:905-907.
- Kaufman DA, Albelda SM, Sun J, Davies PF. Role of lateral cell-cell border location and extracellular/transmembrane domains in PECAM/CD31

- mechanosensation. *Biochem Biophys Res Commun*. 2004;320:1076-1081.
22. Sun J, Paddock C, Shubert J, et al. Contributions of the extracellular and cytoplasmic domains of platelet-endothelial cell adhesion molecule-1 (PECAM-1/CD31) in regulating cell-cell localization. *J Cell Sci*. 2000;113:1459-1469.
  23. Lu TT, Yan LG, Madri JA. Integrin engagement mediates tyrosine dephosphorylation on platelet-endothelial cell adhesion molecule 1. *Proc Natl Acad Sci U S A*. 1996;93:11808-11813.
  24. Gratzinger D, Canosa S, Engelhardt B, Madri JA. Platelet endothelial cell adhesion molecule-1 modulates endothelial cell motility through the small G-protein Rho. *FASEB J*. 2003;17:1458-1469.
  25. O'Brien CD, Cao G, Makrigiannakis A, DeLisser HM. Role of immunoreceptor tyrosine-based inhibitory motifs of PECAM-1 in PECAM-1-dependent cell migration. *Am J Physiol Cell Physiol*. 2004;287:C1103-C1113.
  26. Osawa M, Masuda M, Harada N, Lopes RB, Fujiwara K. Tyrosine phosphorylation of platelet endothelial cell adhesion molecule-1 (PECAM-1, CD31) in mechanically stimulated vascular endothelial cells. *Eur J Cell Biol*. 1997;72:229-237.
  27. Osawa M, Masuda M, Kusano K, Fujiwara K. Evidence for a role of platelet endothelial cell adhesion molecule-1 in endothelial cell mechanosignal transduction: is it a mechanoresponsive molecule? *J Cell Biol*. 2002;158:773-785.
  28. Ilan N, Cheung L, Pinter E, Madri JA. Platelet-endothelial cell adhesion molecule-1 (CD31), a scaffolding molecule for selected catenin family members whose binding is mediated by different tyrosine and serine/threonine phosphorylation. *J Biol Chem*. 2000;275:21435-21443.
  29. Biswas P, Canosa S, Schoenfeld D, et al. PECAM-1 affects GSK-3 $\beta$ -mediated beta-catenin phosphorylation and degradation. *Am J Pathol*. 2006;169:314-324.
  30. Smythe WR, Hwang HC, Amin KM, et al. Use of recombinant adenovirus to transfer the herpes simplex virus thymidine kinase (HSVtk) gene to thoracic neoplasms: an effective in vitro drug sensitization system. *Cancer Res*. 1994;54:2055-2059.
  31. DeLisser HM, Chilkotowsky J, Yan HC, Daise ML, Buck CA, Albelda SM. Deletions in the cytoplasmic domain of platelet-endothelial cell adhesion molecule-1 (PECAM-1, CD31) result in changes in ligand binding properties. *J Cell Biol*. 1994;124:195-203.
  32. O'Brien CD, Lim P, Sun J, Albelda SM. PECAM-1-dependent neutrophil transmigration is independent of monolayer PECAM-1 signaling or localization. *Blood*. 2003;101:2816-2825.
  33. Jackson DE, Kupcho KR, Newman PJ. Characterization of phosphotyrosine binding motifs in the cytoplasmic domain of platelet/endothelial cell adhesion molecule-1 (PECAM-1) that are required for the cellular association and activation of the protein-tyrosine phosphatase, SHP-2. *J Biol Chem*. 1997;272:24868-24875.
  34. Yan HC, Pilewski JM, Zhang Q, DeLisser HM, Romer L, Albelda SM. Localization of multiple functional domains on human PECAM-1 (CD31) by monoclonal antibody epitope mapping. *Cell Adhes Commun*. 1995;3:45-66.
  35. Muro S, Gajewski C, Koval M, Muzykantov VR. ICAM-1 recycling in endothelial cells: a novel pathway for sustained intracellular delivery and prolonged effects of drugs. *Blood*. 2005;105:650-658.
  36. Etienne-Manneville S, Hall A. Rho GTPases in cell biology. *Nature*. 2002;420:629-635.
  37. Tzima E. Role of small GTPases in endothelial cytoskeletal dynamics and the shear stress response. *Circ Res*. 2006;98:176-185.
  38. Romer LH, McLean NV, Yan HC, Daise M, Sun J, DeLisser HM. IFN- $\gamma$  and TNF- $\alpha$  induce redistribution of PECAM-1 (CD31) on human endothelial cells. *J Immunol*. 1995;154:6582-6592.
  39. Newman PJ. The biology of PECAM-1. *J Clin Invest*. 1997;100(Suppl):S25-S29.
  40. Scalia R, Lefer AM. In vivo regulation of PECAM-1 activity during acute endothelial dysfunction in the rat mesenteric microvasculature. *J Leukoc Biol*. 1998;64:163-169.
  41. Muro S, Koval M, Muzykantov V. Endothelial endocytic pathways: gates for vascular drug delivery. *Curr Vasc Pharmacol*. 2004;2:281-299.
  42. Muro S, Cui X, Gajewski C, Murciano JC, Muzykantov VR, Koval M. Slow intracellular trafficking of catalase nanoparticles targeted to ICAM-1 protects endothelial cells from oxidative stress. *Am J Physiol Cell Physiol*. 2003;285:C1339-C1347.
  43. Newman PJ, Newman DK. Signal transduction pathways mediated by PECAM-1: new roles for an old molecule in platelet and vascular cell biology. *Arterioscler Thromb Vasc Biol*. 2003;23:953-964.
  44. Harada N, Masuda M, Fujiwara K. Fluid flow and osmotic stress induce tyrosine phosphorylation of an endothelial cell 128 kDa surface glycoprotein. *Biochem Biophys Res Commun*. 1995;214:69-74.
  45. Newton-Nash DK, Newman PJ. A new role for platelet-endothelial cell adhesion molecule-1 (CD31): inhibition of TCR-mediated signal transduction. *J Immunol*. 1999;163:682-688.
  46. Flaszewski H, Reth M. Dual role of the tyrosine activation motif of the Ig- $\alpha$  protein during signal transduction via the B cell antigen receptor. *EMBO J*. 1994;13:83-89.
  47. Hall A, Nobes CD. Rho GTPases: molecular switches that control the organization and dynamics of the actin cytoskeleton. *Philos Trans R Soc Lond B Biol Sci*. 2000;355:965-970.
  48. Wang Y, Sheibani N. PECAM-1 isoform-specific activation of MAPK/ERKs and small GTPases: implications in inflammation and angiogenesis. *J Cell Biochem*. 2006;98:451-468.
  49. Shikata Y, Rios A, Kawkitinarong K, DePaola N, Garcia JG, Birukov KG. Differential effects of shear stress and cyclic stretch on focal adhesion remodeling, site-specific FAK phosphorylation, and small GTPases in human lung endothelial cells. *Exp Cell Res*. 2005;304:40-49.
  50. Kaunas R, Nguyen P, Usami S, Chien S. Cooperative effects of Rho and mechanical stretch on stress fiber organization. *Proc Natl Acad Sci U S A*. 2005;102:15895-15900.
  51. Worthylake RA, Burridge K. Leukocyte transendothelial migration: orchestrating the underlying molecular machinery. *Curr Opin Cell Biol*. 2001;13:569-577.
  52. Lusinskas FW, Ma S, Nusrat A, Parkos CA, Shaw SK. The role of endothelial cell lateral junctions during leukocyte trafficking. *Immunol Rev*. 2002;186:57-67.
  53. Stevens T, Garcia JG, Shasby DM, Bhattacharya J, Geiger B. Spatial and temporal relationships between cadherins and PECAM-1 in cell-cell junctions of human endothelial cells. *J Cell Biol*. 1994;126:247-258.
  54. Matsumura T, Wolff K, Petzelbauer P. Endothelial cell tube formation depends on cadherin 5 and CD31 interactions with filamentous actin. *J Immunol*. 1997;158:3408-3416.
  55. Mamdouh Z, Chen X, Pierini LM, Maxfield FR, Muller WA. Targeted recycling of PECAM from endothelial surface-connected compartments during diapedesis. *Nature*. 2003;421:748-753.
  56. Muzykantov VR. Biomedical aspects of targeted delivery of drugs to pulmonary endothelium. *Expert Opin Drug Deliv*. 2005;2:909-926.
  57. Valadon P, Garnett JD, Testa JE, Bauerle M, Oh P, Schnitzer JE. Screening phage display libraries for organ-specific vascular immunotargeting in vivo. *Proc Natl Acad Sci U S A*. 2006;103:407-412.
  58. Mahooti S, Graesser D, Patil S, et al. PECAM-1 (CD31) expression modulates bleeding time in vivo. *Am J Pathol*. 2000;157:75-81.
  59. Graesser D, Solowiej A, Bruckner M, et al. Altered vascular permeability and early onset of experimental autoimmune encephalomyelitis in PECAM-1-deficient mice. *J Clin Invest*. 2002;109:383-392.
  60. Maas M, Stapleton M, Bergom C, Mattson DL, Newman DK, Newman PJ. Endothelial cell PECAM-1 confers protection against endotoxin shock. *Am J Physiol Heart Circ Physiol*. 2005;288:H159-H164.
  61. Carrithers M, Tandon S, Canosa S, Michaud M, Graesser D, Madri JA. Enhanced susceptibility to endotoxin shock and impaired STAT3 signaling in CD31-deficient mice. *Am J Pathol*. 2005;166:185-196.
  62. Perkowski S, Scherperle A, Murciano JC, et al. Dissociation between alveolar transmigration of neutrophils and lung injury in hyperoxia. *Am J Physiol Lung Cell Mol Physiol*. 2006;291:L1050-L1058.